Comparison of senescence-related changes between three- and two-dimensional cultured adipose-derived mesenchymal stem cells

Qiliang Yin
Jilin University Norman Bethune Health Science Center

Na Xu
Jilin Medical University

Dong sheng Xu
Jilin University First Hospital

Ming xin Dong
Institute of military veterinary medicine, academy of military medical sciences

Xiu min Shi
Jilin University First Hospital

Yan Wang
Institute of military veterinary midecine, Academy of military medical sciences

Zhuo Hao
Institute of military veterinary medicine, academy of military medical sciences

Shuang shuang Zhu
Jilin University First Hospital

Dong hai Zhao
Jilin Medical University

Hao fan Jin
Cancer Center at the First Hospital of Jilin University

Wen sen Liu
Institute of military veterinary medicine, academy of military medical sciences

Research

Keywords: Adipose-derived mesenchymal stem cells, three-dimensional culture, senescence, energy metabolism

---

Abstract

Background: Adipose-derived mesenchymal stem cells (ADMSCs) have attracted widespread interest as cell-based tissue repair systems. To obtain adequate quantities of ADMSCs for therapeutic applications, extensive in vitro expansion is required. However, under current two-dimensional (2D) approaches , ADMSCs rapidly undergo replicative senescence , and cell growth is impeded and stem cell properties are eliminated by mechanisms that are poorly understood . These issues limit the extensive applications of ADMSCs . In this study, we investigated senescence-related changes in mesenchymal stem cells (MSCs) isolated from human adipose tissue in 2D and three-dimensional (3D) cultures.

Methods: We studied cell growth over a given period (21 days) to determine if modes of culture were associated with ADMSCs senescence . ADMSCs were isolated from healthy females by liposuction surgery and then were grew in 2D and 3D cultures. The cell morphology was observed during cell culture. Every other time of culture, senescence-associated β-galactosidase (SA-β-gal) expression, cell viability, proliferation, and differentiation potential of ADMSCs from 2D and 3D cultures were detected. Also, senescence and stemness related genes expression, telomere length, telomerase activity, and energy metabolism of ADMSCs for different culture time were evaluated.

Results: With long-term propagation, we observed significant changes in cell morphology, proliferation, differentiation abilities and energy metabolism, which were associated with increases in SA-β-gal activity, and decreases in telomere length and telomerase activity . Notably, when cultured in 3D, these changes were improved.

Conclusions: Our results indicate that 3D culture is able to ameliorate senescence-related changes in ADMSCs.

Background

Mesenchymal stem cells (MSCs) are pluripotent stem cells with the potential to self-replicate and multi-differentiate[1,2]. Adipose tissue is an important source of MSCs[3]. Adipose-derived mesenchymal stem cells (ADMSCs) are harvested with low donor-site morbidity, and are not associated with ethical issues, therefore, they represent promising candidates for various clinical applications, including tissue repair and regenerative medicine[2,4]. In recent years, ADMSCs have been shown to promote revascularization, activate local stem cell niches, reduce oxidative stress and modulate immune responses[3,5]. However, therapies utilizing ADMSCs often require ex vivo expansion to generate large quantities of cells required for patients[6,7]. Therefore, in vitro expansion is particularly important for ADMSCs.

Two-dimensional (2D) culture has been routinely used over the past several decades[8]. Typically, MSCs are expanded on stiff tissue culture-treated polystyrene, as a 2D monolayer[6]. However, growing cells in flat layers on plastic surfaces do not accurately mimic the natural in vivo cellular microenvironment, due to a lack of three-dimensional cues from the external media[9]. Moreover, the cellular microenvironment

can seriously influence MSCs characteristics and cause issues when transferring basic research to clinical settings[10]. Accumulating evidence indicates that extensive passaging of ADMSCs in 2D culture induces replicative senescence, resulting in cell cycle arrest, cell morphology and metabolic changes, and loss of differentiation potential[11-14]. Therefore, ADMSCs are prone to senescence, and are difficult to maintain during long-term 2D expansion[15]. As a result, efforts have led to the development of novel approaches to recreate more physiologically relevant environments in the form of three-dimensional (3D) culture[16,17].

3D culture is a simple and effective culture system, developed on the basis of a 2D monolayer, but with *in vivo* animal model characteristics[18,19]. Currently, 3D culture systems are gaining interest with regard to recreating complex extracellular microenvironments (ECM), thereby providing insights into conditions experienced by MSCs. When compared to 2D approaches, 3D culture creates an artificial ECM where cells grow or interact with their surroundings in three dimensions[8,20]. In such cultures, there is increased MSCs communication with neighboring cells, and cell-to-cell and cell-to-matrix connections are easily formed[21]. Reports from the literature suggest that 3D culture of human umbilical cord MSCs promotes cell yields, maintain stemness, and represents a promising strategy for cell expansion on industrial levels, with great potential for cell therapy and biotechnology[22-24]. Additionally, 3D microenvironments encourage MSCs growth and differentiation into hepatocyte-like cells, in the presence of growth factors[25]. More importantly, the utilization of 3D culture techniques circumvents issues surrounding altered cellular properties of extensively expanded MSCs[7,21]. In this work, we focus on the benefits of using 3D cultures, and investigate ideal and optimized living environments for ADMSCs growth *in vitro*.

Methods

Isolation and cultivation of human ADMSCs

Abdominal adipose tissue was obtained from five healthy females by liposuction surgery. Lipoaspirate MSCs were isolated and characterized as previously described[26]. Cells in culture were maintained at 37°C with 5% CO_2, until 80% cell confluence, then cells were passaged on. ADMSCs from the third passage were plated in conventional 2D or 3D culture vessels. For 2D culture, cells from third passage were cultured in six-well plates at 1×10^6 cells/ml. Hydrogel (The well bioscience, Catalogue No. TWG002,Shanghai,China), as a non-animal derived polysaccharide hydrogel system that mimics the natural cellular microenvironment, is a new synthetic biomaterial for cell expansion *in vitro*, and is the main constituent of 3D culture. The hydrogel was mixed with cell culture medium to form a hydrogel matrix. The dilution ratio was 1:1, i.e., Hydrogel: PBS, 1:1, v/v. The hydrogel and ADMSCs were uniformly mixed and were seeded into a six-well plate at 1×10^6 cells/ml as the 3D culture. Then, the cell culture medium (DAKEWE, EliteGro^{TM} -Adv, Beijing, China) was added to cover the hydrogel carefully. The medium was replaced every three days. When ADMSCs grew to 80% confluence, the cells were passaged at 1፥2. It was a little different for cells passage of 3D culture. Firstly, preheated 0.1× PBS and empty centrifuge tube in 37°C water bath before took out the cell culture plate from incubator. Discarded the medium covered with the top of the hydrogel, added 1 ml of pre-heated 0.1× PBS into each hole and

thoroughly mixed. Then, put the mixture into the pre-heated centrifuge tube and rinsed each hole with 1 ml preheated 0.1× PBS, and added pre-heated 0.1× PBS to 10ml, thoroughly mixed. Finally, collected the cells after centrifuging at 1000 rpm for 5 minutes. ADMSCs were reseeded at six-well plate.

The first day (d 1) was defined when ADMSCs from the third passage were seeded into six-well plates, as described.

Characterization of ADMSCs

Flow cytometry assessment was conducted to confirm the mesenchymal origin of cells. Third passage cells were resuspended following digestion with 0.125% trypsin. A minimum of $1×10^5$ cells/ml were collected from six-well plates. Rat monoclonal anti-human antibodies were used at a dilution of 1:150 for all cell surface markers. MSCs were incubated with phycoerythrin (PE)-coupled antibodies, CD34 (sc-7324; Santa Cruz) and CD45 (554,878; BD Biosciences), and fluorescein isothiocyanate (FITC)-coupled antibodies, CD44 (550,974; BD Biosciences) and CD105 (BD Biosciences), in the dark at room temperature for 30 min. IgG1-PE and IgG1-FITC were used as isotype controls. Cell data were analyzed using Paint-A-Gate Pro™ software.

Senescence-associated (SA)-β-galactosidase (Gal) assay

ADMSCs from 2D and 3D cultures at 3 d, 7 d, 14 d and 21 d, were seeded in six-well plates at $1×10^5$ cells/well overnight. The next day, cells were fixed for 30 min at room temperature in 4% formaldehyde, and washed twice in PBS (pH 7.3). Then, ADMSCs were incubated overnight at 37°C with freshly prepared SA-β-Gal stain solution (C0602, Beyotime, Shanghai, China) following manufacturer's instructions. At least 400 cells were observed in randomly chosen, non-overlapping fields by three independent observers to quantify SA-β-gal expression. Positive cells were stained blue and counted in three randomly selected fields under the microscope (XPF-550C, caikon, Shanghai, China). The experiment was performed three times, and the mean percentage of cells expressing SA-β-Gal was calculated.

Cell viability

ADMSCs viability was determined using Muse Count & Viability Assay in the Muse Cell Analyzer (Luminex, USA) according to manufacturer's instructions. Cells ($1×10^6$ cells/well) were harvested from both 2D and 3D cultures. They were then resuspended in medium to achieve a cell density of $2×10^5$ cells/ml, from which 50 μl cells and 450 μl Muse™ count & viability reagent were added to a tube, and incubated for 5 min in the dark at room temperature. Cell viability was evaluated by miniaturized fluorescence detection and microcapillary cytometry with Muse Cell Analyzer. In addition, we counted the cells in 2D and 3D cultures at every measured time point by Muse Cell Analyzer.

Stain of living cells

ADMSCs from 2D and 3D cultures at 3 d, 7 d, 14 d and 21 d, were stained by HCS NuclearMask™ Blue Stain (H10325, Invitrogen, Shanghai, China) according to manufacturer's instructions. The cells were

pulsed with 100μl staining solution (1:2000) for 30min at room temperature. After the incubation, the stained cells

were analyzed by fluorescence microscopy (IX71, OLYMPUS, Xiameng, China).

Adipo- and osteogenic differentiation of ADMSCs

ADMSCs from 3 d, 7 d, 14 d and 21 d were induced to undergo adipogenic and osteogenic differentiation, to identify cell capacity for differentiation in 2D and 3D cultures. For adipogenic differentiation, ADMSCs were seeded in 24-well plates at a density of 1×10^5 cells/well. MSCgo™ adipogenic differentiation medium (Catalogue No. 05412, STEMCELL, USA) was used to induce adipogenic differentiation after cells reached 95% confluence. Induction/maintenance media was replaced for cycles of three days/one day, respectively. Differentiated cells were assessed by staining intracellular lipid droplets with Oil Red O (MC37A0-1.4, VivaCell BIOSCIENCES, Shanghai, China) after 21 days in adipogenesis induction medium. For osteogenic differentiation, a similar process was adopted. MSCgo™ osteogenic differentiation medium (Catalogue No. 05465, STEMCELL, USA) induced osteogenic differentiation when cells reached 95% confluence. Differentiated cells were stained using Alizarin Red S (MC37C0-1.4, VivaCell BIOSCIENCES, Shanghai, China) staining of accumulated calcium deposits, after 28 days of differentiation. At least 300 cells were observed in randomly chosen, non-overlapping fields by three independent observers to quantify cells differentiation capacity. Positive cells were counted in three randomly selected fields under the microscope (XPF-550C, caikon, Shanghai, China).

Real-time fluorescence quantitative polymerase chain reaction (RT-qPCR)

Total RNA was isolated from ADMSCs using TRIzol reagent (Invitrogen, USA) following manufacturer's instructions. cDNA was prepared by reverse transcription using the PrimeScript™ RT-PCR Kit (TaKaRa, Japan). Next, mRNA levels were quantified for aging-related genes (p16, p21, p53) and stemness-related genes (Sox2, Oct4, Nanog, c-myc) by RT-qPCR on an ABI Prism7900 Detector (Applied Biosystems, USA), using SYBR Premix Ex Taq™. β-actin was used as a reference gene. Each experimental group was analyzed in triplicate. mRNA expression was calculated using the $2^{-\Delta\Delta Ct}$ method. Primer sequences for RT-qPCR are shown (Table 1).

Telomere length and activity assay

Genomic DNA (gDNA) was isolated from ADMSCs and used as a template for RT-qPCR. The relative telomere length of ADMSCs from 3 d, 7 d, 14 d and 21 d was assayed using the relative human telomere length quantification RT-qPCR assay kit (Catalogue No. 8908, ScienCell, USA) following manufacturer's instructions. Data were analyzed using the comparative quantification cycle value (ΔΔCq) method. Telomeres are maintained by telomerase, which comprises telomerase reverse transcriptase (TERT) and telomerase RNA component (TERC)[27]; thus, TERT expression is consistent with telomerase activity. The RT-qPCR assay indirectly reflects telomerase activity by detecting TERT mRNA expression levels. The procedure was identical to the above.

Relative mitochondrial DNA copy number quantification

Mitochondrial DNA (mtDNA) from ADMSCs was used as a template for RT-qPCR. The relative mtDNA copy number of ADMSCs from different time points was determined using the relative human mtDNA copy number quantification RT-qPCR assay kit (Catalogue No. 8938, ScienCell, USA) following manufacturer's instructions. Data were analyzed using the comparative $\Delta\Delta Cq$ method.

Cellular energy metabolism studies

The extracellular acidification rate (ECAR) and oxygen consumption rate (OCR) of cells were detected using the XF96 extracellular flux analyzer (Seahorse Bioscience; North Billerica, MA, USA) following manufacturer's instructions. ADMSCs were seeded at 5×10^3 cells/well in a 96-well Seahorse culture plate (Seahorse Bioscience, North Billerica, MA, USA), before conducting the experiment. For the ECAR assay, studies were performed in un-buffered DMEM (Catalogue No. 11965092, Gibco^{TM}, USA), pH 7.3 at 37°C. Glucose (8 mM), oligomycin A (oligo; an ATP synthase inhibitor, 0.8 µM) and 2-deoxyglucose (2-DG; inhibitor of glycolysis; 80 mM) were added to different ports of the Seahorse cartridge. For OCR assays, analyses were conducted in medium consisting of 20 mM glucose, 1.8 mM sodium pyruvate in un-buffered DMEM, pH 7.3, at 37°C. Oligomycin A (1 µM), carbonyl cyanide m-chlorophenylhydrazone (FCCP; a mitochondrial uncoupler; 400 nM), rotenone (complex I inhibitor; 0.8 µM) and antimycin A (complex III inhibitor; 0.8 µM) were added to different ports of the Seahorse cartridge. Each experimental group was assayed with four to five replicates in each analysis. ECAR and OCR data were normalized to cell numbers, as detected by CellTiter-Glo analysis (Promega, USA) at assay end.

Statistical data analysis

Numerical data were reported using means ± standard deviation (SD). Data analyses were performed using paired t-tests with GraphPad Prism 7 software. Statistical differences were assessed at $p < 0.05$, $p < 0.01$, $p < 0.001$.

Results

Morphological characteristics of ADMSCs

Primary ADMSCs from culture are shown (Additional file 1: Fig. S1). These cells exhibited fibroblast-like, spindle-shaped morphology, were spiral shaped, and in alignment.

ADMSCs from the third passage were characterized by flow cytometry, indicating the presence of CD34 and CD45 negative (0.89%) surface markers (Additional file 2: Fig. S2a), and CD44 and CD105 positive (99.49%) surface markers (Additional file 2: Fig. S2b).

As described, ADMSCs from the third passage were plated in 2D and 3D culture (Additional files 3: Fig. S3), and photographed at 3 d, 7 d, 14 d and 21 d (Fig. 1). Cell morphology varied with different time points, and culture modes. In 2D culture, cells showed a fibroblast-like morphology, were spindle-shaped,

and in alignment. At 3 d and 7 d, they were relatively homogeneous; cells had the characteristic spindle-shape and the cell surface appeared smooth (Fig. 1a, 1b). At 14 d, 2D cultured cells still maintained the characteristic MSCs shape, however, some cells displayed pseudopod-like structures, i.e., they were longer and flatter (Fig. 1c). Unlike 3 d and 7 d, cell shape at 21 d was flat, and almost all ADMSCs had lost their MSCs shape; i.e., cells were focally aggregated and exhibited a "fried egg" morphology (Fig. 1d).

In contrast, there were no morphological variations in 3D culture, ADMSCs grew in a hydrogel suspension, and most cells were round in shape, with a gradually decreasing cell density in relation to time points (Fig. 1e–1h).

In addition, ADMSCs were retrieved and re-cultured in six-well plates, without hydrogel after 3D culture for 3 d, 7 d, 14 d and 21 d. Although cell shape gradually became longer and flatter as time progressed, most cells maintained elongated spindle-shapes and smooth cell surfaces. More importantly, cells never lost their characteristic MSCs shape (Fig. 1i–1l).

Evaluating senescence-associated (SA) β-Galactosidase (Gal) expression

ADMSCs from 2D and 3D cultures were stained with SA-β-Gal. Aging cells stained blue reflected SA-β-gal expression. As anticipated, little or no expression was observed at 3 d and 7 d in 2D and 3D cultures, but subsequent increases in expression were observed with cultivation times. While cell senescence was more visible in 2D cells when compared with 3D cells at 14 d and 21 d (Fig. 2a), blue ADMSCs in 2D culture were significantly increased when compared to 3D culture at 14 d (-9.417 ± 0.651). Strikingly, most ADMSCs were stained blue at 21 d in 2D cultures, but limited cell densities were stained blue in 3D culture (26.08±0.363), at the same time period (Fig. 2b).

ADMSCs viability

ADMSCs viability was assessed in 2D and 3D cultures at different time points (Fig. 3a). As expected, ADMSCs viability was comparable at 3 d and 7 d under both culture conditions, and highest viability appeared at 7 d. However, viability decreased was observed at 14 d and 21 d, and was significantly decreased in 2D cultures when compared with 3D. Significantly, cells viability in 3D culture was greater than in 2D cultures at 14 d (7.933±1.281), and 21 d (6.133±1.255) (Fig. 3b). Meanwhile, ADMSCs number in 2D and 3D cultures at every measured time point was counted (Fig. 3c). Cells number was significantly increased within 7 d in 2D and 3D cultures, and the population doubling time was 6 d and 4 d respectively, subsequently, number of cells decreased rapidly, especially in 2D culture. Obviously, the cells number in 3D cultures was significantly greater than that in 2D (0.586±0.411). Additionally, analysis of ADMSCs staining showed that the number of living cells in 2D and 3D cultures was basically in accordance with the result of cells viability (Fig. 3d).

Adipo- and osteogenic differentiation of ADMSCs

Differences in adipo- and osteogenic capacities of ADMSCs in 2D and 3D cultures over the time points, 3 d, 7 d, 14 d and 21 d were analyzed (Fig. 3e, 3f). Whether in 2D or 3D culture, the adipo- and osteogenic

differentiation potential of ADMSCs were similar at 3 d and 7 d. However, an obvious age-related decline was observed in adipo- and osteogenic differentiation capacity for ADMSCs at 14 d (13.58±2.184, 12.75±3.031, respectively) and 21 d (11.58±2.309, 10.95±2.282, respectively) (Fig. 3g, 3h) in 2D cultures. Notably in this culture, ADMSCs nearly lost osteogenic differentiation at 21 d (Fig. 3h).

Evaluating aging- and stemness-related gene expression

Changes in aging- and stemness-related gene expression were evaluated by quantifying mRNA levels in ADMSCs from both culture conditions. As expected, the expression of age-related genes p16, p21 and p53 was gradually increased with culture time, furthermore, gene expression in ADMSCs from 2D culture were significantly higher than 3D cultures at 14 d (-0.767±0.169,-0.559±0.019, 0.351±0.023, respectively) and 21 d (-1.009±0.178, -0.975±0.014, -0.947±0.203, respectively). Conversely, the expression levels of stemness-related genes, Sox2, Oct4, Nanog and c-myc exhibited a decreasing tendency with long-term expansion. Moreover, Oct4 and Nanog expression exhibited a more significant reduction in 2D culture than 3D cultures at 14 d (0.998±0.021, 0.921±0.068, respectively) and 21 d (0.695±0.201, 0.997±0.307, respectively), besides, Sox2 and c-myc expression were significantly decreased in 2D cultures at 21 d (0.693±0.125, 0.616±0.143, respectively) (Fig. 4).

Evaluation of relative telomere length, telomerase activity and relative mitochondrial DNA copy number

We identified that telomere length in ADMSCs gradually shortened during cell expansion in both 2D and 3D cultures. However, telomere length shortened significantly more in 2D culture when compared to 3D, especially for 14 d (0.274±0.047) and 21 d (0.223±0.0052). It seemed that the decline fluctuation of telomere length was steadier in 3D culture (Fig. 5a). In addition, TERT expression revealed that changes in telomerase activity agreed with relative telomere lengths in ADMSCs (Fig. 5b). Similarly, relative mtDNA copy numbers of ADMSCs in 2D and 3D cultures were gradually decreased, but mtDNA copy numbers in 3D culture were significantly higher when compared with 2D cultures at 14 d (0.315±0.043) and 21 d (0.349±0.055) (Fig. 5c).

Changes in energy metabolism in ADMSCs

We analyzed the effects of 3D and 2D culture on ADMSCs energy metabolism (Fig. 6a).
It is generally accepted that glycolysis and mitochondrial respiration are two major energy production pathways in cells[28,29]. Through glycolysis, ADMSCs utilize glucose to generate lactate; thus, if cells are compromised, increased lactate levels could create an acidic environment, as assessed by ECAR[30], and increased OCR is an indicator of mitochondrial respiration. We observed that ECAR level in ADMSCs in 3D cultures were higher than 2D cultures at 7 d, 14 d and 21 d (Fig. 6b), but slightly less at 3 d, as ECAR levels showed little differences between 2D and 3D cultures at this early stage. OCR levels of ADMSCs in 3D culture were higher when compared with 2D culture, at each time point (Fig. 6c). Taken together, the 3D culture of ADMSCs appeared to induce positive regulation of glycolysis and mitochondrial respiration, i.e., 3D cultures sustained energy metabolism stability in ADMSCs.

Discussion

Human ADMSCs are ideal candidates for diverse regenerative medicine approaches and tissue engineering strategies[31,32]. However, it is interesting that therapies requiring ADMSCs often require *ex vivo* expansion approaches to generate the large numbers of cells required for patients, and to overcome cell senescence limitations[6,33]. It is widely recognized that 3D cultures create a pragmatic ECM, and mimic *in vivo* development[20,34]. Therefore, 3D culture of MSCs could increase cell yields, enhance differentiation, maintain stemness and provide promising strategies for MSCs expansion on an industrial scale, with great potential for cell therapy and biotechnology[20,22].

In terms of morphological and biochemical characteristics, *in vitro* MSCs senescence is characterized by an enlarged flat cellular morphology, increased SA-β-gal activity, increased expression of p16, p21 and p53[12,35], and a loss of stem cell properties[36]. Studies have reported that MSCs enter replicative senescence after extensive culture, leading to morphological and functional cellular changes[23,37]. Cells senescence is a major factor that affects the proliferation and multi-lineage potential of MSCs[23,38]. Here, we discovered that proliferation and adipogenic and osteogenic differentiation in ADMSCs steadily declined following extensive expansion, but notably, the decline in 2D culture was greater than 3D. In addition, 3D ADMSCs at different culture times were Re-adhering in vessels, without hydrogel, we observed that these cells were morphologically younger when compared with 2D culture cells, at the same time period and more importantly, SA-β-gal expression in these cells (3D) was lower. These observations agreed with the literature showing that significant changes in cell morphology were associated with increased SA-β-gal expression[11]. Such phenomenon has been rarely reported, but our data provides critical evidence that 3D culturing exerts positive effects on senescence-associated changes. Interestingly, recent evidence has indicated that even a short 3D culture of 72 h altered extensively expanded MSCs characteristics[7].

Telomere length and telomerase activity represent cell senescence at the cellular level[39]. Moreover, cell lifespan is directly proportional to telomere length[40]. Thus, telomere shortening more than likely functions as a mechanism implicated in cellular senescence[39,41]. Reports have identified a direct correlation between telomerase activity and stem cell function[37], with telomere attrition contributing to aging.[42] Furthermore, studies have demonstrated that the relative telomere length of ADMSCs decline with long-term passaging[38]. Our study suggests that telomere length and telomerase activity of ADMSCs decline with aging, but may be improved by 3D culture, further confirming that 3D culturing exerts positive effects in delaying senescence in ADMSCs.

Although MSCs aging mechanisms during long-term expansion remain ill-defined, it has been shown that in addition to telomere shortening and telomerase activity reduction inducing senescence, oxygen free radical generation and altered mitochondrial function may have plausible roles in aging[43]. Additionally, previous studies have demonstrated that senescence is associated with metabolic changes in the oxidative state of the cell, and that this process is linked to glycolytic ability and mitochondrial function[11-13], suggesting associations between changes in energy metabolism and senescence. The

metabolic energy changes observed in ADMSCs (in 2D and 3D cultures) in this study reveal that ECAR and OCR levels vary greatly between dimensional cultures, over different cultivation periods. Overall, ECAR and OCR levels were higher in 3D cultures, suggesting that this approach had positive effects on glycolytic function and mitochondrial respiration in ADMSCs. Up to now, ADMSCs energy metabolism research is in its infancy, and relationships between energy metabolism changes and ADMSCs senescence had rarely been reported. Accordingly, this study has preliminarily confirmed that 3D culturing slows ADMSCs senescence, by improving mitochondrial function and energy metabolism.

Indeed, some reports have indicated a direct relationship between mitochondrial dysfunction and stem cell aging[28,44]. In several cell systems, mitochondrial dysfunction leads to respiratory chain dysfunction, which may be the result of mutation accumulation in mtDNA, in line with aging[45]. A critical mechanism underlying mitochondrial dysfunction is the expansion of mutations and deletions in mtDNA[29]. Additionally, these accumulated aging-related mutations and deletions lead to decreased mtDNA copy numbers[29,45]. This study has shown that 3D culturing protects mtDNA in ADMSCs from aging-related impairments, suggesting that 3D cultures improve aging-related mitochondrial dysfunction.

Nevertheless, this study has some limitations. Firstly, some data did not reach statistical significance, which may be the result of lack of enough cell culture time *in vitro*. Similarly, we did not assess chondrogenic differentiation in ADMSCs, since the cells need to form spheroids during chondrogenic differentiation, the diversity in capability of sphere-forming of ADMSCs in 2D and 3D culture has a great influence on chondrogenic differentiation, thus, it is difficult to evaluate chondrogenic differentiation ability of the ADMSCs. Finally, we revealed factors that impeded ADMSCs growth *in vitro*, but an in-depth mechanistic exploration of factors that induce cellular senescence is required in future research.

Conclusions

Taken together, this study confirms that 3D culturing relieves senescence-related changes in ADMSCs and highlights the importance of developing 3D culture approaches for sustained and healthy MSCs growth. There is no doubt that 3D culturing will contribute to effective ADMSCs preparations for cellular therapy, and importantly our findings lay the path for future ADMSCs applications in biomedical research. However, further investigations will be required to fully evaluate the effectiveness and safety of ADMSCs in 3D culture for future *in vivo* therapies.

Abbreviations

ADMSCs: Adipose-derived mesenchymal stem cells; 2D: two-dimensional; MSCs: mesenchymal stem cells; 3D: three-dimensional; SA-β-gal: senescence-associated β-galactosidase; ECM: extracellular microenvironments; RT-qPCR: Real-time fluorescence quantitative polymerase chain reaction; gDNA: genomic DNA; TERT: telomerase reverse transcriptase; TERC: telomerase RNA component; mtDNA: Mitochondrial DNA; ECAR: The extracellular acidification rate; OCR : oxygen consumption rate.

Declarations

Acknowledgments

We thank International Science Editing (http://www.internationalscienceediting. com) for editing this manuscript.

Authors' contributions

Qi-liang Yin, and Na Xu: conception and design, collection and/or assembly of data, data analysis and interpretation, manuscript writing; Hao-fan Jin, and Wen-sen Liu: conception and design, supervision of the study, final approval of manuscript. Dong-sheng Xu, Ming-xin Dong, Xiu-min Shi, and Yan Wang: design, collection and/or assembly of data, data analysis and interpretation, statistical analysis; Zhuo Hao, Shuang-shuang Zhu, and Dong-hai Zhao: collection and/or assembly of data. All authors read and approved the final manuscript.

Funding

This research was supported by the Project Agreement for Science & Technology Development, Jilin Province (No. 20190304027YY) and by the Science and Technology Development Program of Jilin Provincial of China (No. 20190201148JC).

Availability of data and materials

The datasets used and/or analyzed during the current study available from

the corresponding author on reasonable request.

Ethics approval and consent to participate

The use of human tissue was approved by the ethics committee of the

the First Hospital of Jilin University, China (EK Nr. 985/2016, 25 January 2018), and the donor gave written consent.

Consent for publication

Not applicable

Competing interests

The authors declare that they have no competing interests.

References

1. Stoltz JF, de Isla N, Li YP et al. Stem Cells and Regenerative Medicine: Myth or Reality of the 21th Century. Stem cells international 2015;2015:734731.

2. Shingyochi Y, Orbay H, Mizuno H. Adipose-derived stem cells for wound repair and regeneration. Expert Opin Biol Ther 2015;15:1285-92.

3. Luck J, Weil BD, Lowdell M et al. Adipose-Derived Stem Cells for Regenerative Wound Healing Applications: Understanding the Clinical and Regulatory Environment. Aesthetic surgery journal 2019.

4. Mizuno H, Tobita M, Uysal AC. Concise review: Adipose-derived stem cells as a novel tool for future regenerative medicine. Stem Cells 2012;30:804-10.

5. Huang H, Kolibabka M, Eshwaran R et al. Intravitreal injection of mesenchymal stem cells evokes retinal vascular damage in rats. FASEB J 2019:fj201901500R.

6. Hoch AI, Leach JK. Concise review: optimizing expansion of bone marrow mesenchymal stem/stromal cells for clinical applications. Stem Cells Transl Med 2015;4:412.

7. Bartosh TJ, Ylostalo JH. Efficacy of 3D Culture Priming is Maintained in Human Mesenchymal Stem Cells after Extensive Expansion of the Cells. Cells 2019;8.

8. Ravi M, Paramesh V, Kaviya SR et al. 3D cell culture systems: advantages and applications. Journal of cellular physiology 2015;230:16-26.

9. Dutta RC, Dutta AK. Cell-interactive 3D-scaffold; advances and applications. Biotechnology advances 2009;27:334-9.

10. Kouroupis D, Sanjurjo-Rodriguez C, Jones E et al. Mesenchymal Stem Cell Functionalization for Enhanced Therapeutic Applications. Tissue Eng Part B Rev 2019;25:55-77.

11. Stab BR, 2nd, Martinez L, Grismaldo A et al. Mitochondrial Functional Changes Characterization in Young and Senescent Human Adipose Derived MSCs. Front Aging Neurosci 2016;8:299.

12. Fafian-Labora JA, Morente-Lopez M, Arufe MC. Effect of aging on behaviour of mesenchymal stem cells. World J Stem Cells 2019;11:337-46.

13. Macrin D, Alghadeer A, Zhao YT et al. Metabolism as an early predictor of DPSCs aging. Scientific reports 2019;9:2195.

14. Khan H, Mafi P, Mafi R et al. The Effects of Ageing on Differentiation and Characterisation of Human Mesenchymal Stem Cells. Curr Stem Cell Res Ther 2018;13:378-83.

15. Sekiya I, Larson BL, Smith JR et al. Expansion of human adult stem cells from bone marrow stroma: conditions that maximize the yields of early progenitors and evaluate their quality. Stem Cells 2002;20:530-41.

16. Tachibana CY. Stem-cell culture moves to the third dimension. Nature 2018;558:329-31.

17. Liu Z, Tang M, Zhao J et al. Looking into the Future: Toward Advanced 3D Biomaterials for Stem-Cell-Based Regenerative Medicine. Adv Mater 2018;30:e1705388.

18. Antoni D, Burckel H, Josset E et al. Three-dimensional cell culture: a breakthrough in vivo. International journal of molecular sciences 2015;16:5517-27.

19. Haycock JW. 3D cell culture: a review of current approaches and techniques. Methods in molecular biology 2011;695:1-15.

20. Luo Y, Lou C, Zhang S et al. Three-dimensional hydrogel culture conditions promote the differentiation of human induced pluripotent stem cells into hepatocytes. Cytotherapy 2018;20:95-107.

21. Cesarz Z, Tamama K. Spheroid Culture of Mesenchymal Stem Cells. Stem Cells Int 2016;2016:9176357.

22. Li Y, Guo G, Li L et al. Three-dimensional spheroid culture of human umbilical cord mesenchymal stem cells promotes cell yield and stemness maintenance. Cell Tissue Res 2015;360:297-307.

23. Truong NC, Bui KH, Van Pham P. Characterization of Senescence of Human Adipose-Derived Stem Cells After Long-Term Expansion. Advances in experimental medicine and biology 2018.

24. Bae YJ, Kwon YR, Kim HJ et al. Enhanced differentiation of mesenchymal stromal cells by three-dimensional culture and azacitidine. Blood Res 2017;52:18-24.

25. El-Hamid SA, Mogawer A. In vitro mesenchymal stem cells differentiation into hepatocyte-like cells in the presence and absence of 3D microenvironment. Comparative Clinical Pathology 2013;23:1051-8.

26. Gutiérrez ML, Guevara JM, Echeverri OY et al. Aggrecan catabolism during mesenchymal stromal cell in vitro chondrogenesis. Animal Cells and Systems 2013;17:243-9.

27. Fajkus J, Sykorova E, Leitch AR. Telomeres in evolution and evolution of telomeres. Chromosome Res 2005;13:469-79.

28. Bratic A, Larsson NG. The role of mitochondria in aging. J Clin Invest 2013;123:951-7.

29. Greaves LC, Nooteboom M, Elson JL et al. Clonal expansion of early to mid-life mitochondrial DNA point mutations drives mitochondrial dysfunction during human ageing. PLoS Genet 2014;10:e1004620.

30. Zhang B, Wu J, Cai Y et al. AAED1 modulates proliferation and glycolysis in gastric cancer. Oncol Rep 2018;40:1156-64.

31. Choudhery MS, Badowski M, Muise A et al. Donor age negatively impacts adipose tissue-derived mesenchymal stem cell expansion and differentiation. Journal of translational medicine 2014;12:8.

32. Jin HJ, Bae YK, Kim M et al. Comparative analysis of human mesenchymal stem cells from bone marrow, adipose tissue, and umbilical cord blood as sources of cell therapy. International journal of molecular sciences 2013;14:17986-8001.

33. Stolzing A, Jones E, McGonagle D et al. Age-related changes in human bone marrow-derived mesenchymal stem cells: consequences for cell therapies. Mech Ageing Dev 2008;129:163-73.

34. Madl CM, LeSavage BL, Dewi RE et al. Matrix Remodeling Enhances the Differentiation Capacity of Neural Progenitor Cells in 3D Hydrogels. Advanced Science 2019;6.

35. Zhang M, Du Y, Lu R et al. Cholesterol Retards Senescence in Bone Marrow Mesenchymal Stem Cells by Modulating Autophagy and ROS/p53/p21(Cip1/Waf1) Pathway. Oxid Med Cell Longev 2016;2016:7524308.

36. Tobita M, Tajima S, Mizuno H. Adipose tissue-derived mesenchymal stem cells and platelet-rich plasma: stem cell transplantation methods that enhance stemness. Stem cell research & therapy 2015;6:215.

37. Drela K, Stanaszek L, Nowakowski A et al. Experimental Strategies of Mesenchymal Stem Cell Propagation: Adverse Events and Potential Risk of Functional Changes. Stem Cells Int 2019;2019:7012692.

38. Legzdina D, Romanauska A, Nikulshin S et al. Characterization of Senescence of Culture-expanded Human Adipose-derived Mesenchymal Stem Cells. Int J Stem Cells 2016;9:124-36.

39. Saretzki G. Telomeres, Telomerase and Ageing. Subcell Biochem 2018;90:221-308.

40. Alrefaei GI, Alkarim SA, Abduljabbar HS. Impact of Mothers' Age on Telomere Length and Human Telomerase Reverse Transcriptase Expression in Human Fetal Membrane-Derived Mesenchymal Stem Cells. Stem cells and development 2019.

41. Funayama R, Ishikawa F. Cellular senescence and chromatin structure. Chromosoma 2007;116:431-40.

42. Yu KR, Kang KS. Aging-related genes in mesenchymal stem cells: a mini-review. Gerontology 2013;59:557-63.

43. Romano AD, Serviddio G, de Matthaeis A et al. Oxidative stress and aging. J Nephrol 2010;23 Suppl 15:S29-36.

44. Fellous TG, Islam S, Tadrous PJ et al. Locating the stem cell niche and tracing the hepatocyte lineages in human liver. Hepatology 2009;49:1655-63.

45. Miquel J, Economos AC, Fleming J et al. Mitochondrial role in cell aging. Exp Gerontol 1980;15:575-91.

Additional Files

Additional file 1: Fig. S1 ADMSCs exhibit fibroblast-like, spindle-shaped morphology, were spiral shaped and in alignment.

Additional file 2: Fig. S2 Flow cytometry analysis showing the presence of CD34 and CD45 negative (0.89%) surface markers **(a)**, and CD44 and CD105 positive (99.49%) surface markers **(b)**.

Additional file 3: Fig. S3 Model graph of 3D hydrogel culture.

Table

Table 1 Primers used for RT-qPCR

Gene	Primer sequence (5¢-3¢)	Product size (bp)
β-actin	Forward: CATGTACGTTGCTATCCAGGC	250
	Reverse: CTCCTTAATGTCACGCACGAT	
P16	Forward: ATCATCAGTCACCGAAGG	369
	Reverse: TCAAGAGAAGCCAGTAACC	
P21	Forward: CATCTTCTGCCTTAGTCTCA	163
	Reverse: CACTCTTAGGAACCTCTCATT	
P53	Forward: CGGACGATATTGAACAATGG	158
	Reverse: GGAAGGGACAGAAGATGAC	
SOX2	Forward: GCCGAGTGGAAACTTTTGTCG	155
	Reverse: GGCAGCGTGTACTTATCCTTCT	
OCT4	Forward: CTGGGTTGATCCTCGGACCT	243
	Reverse: CCATCGGAGTTGCTCTCCA	
Nanog	Forward: TCTATAACTGTGGAGAGGAATC	122
	Reverse: GGTCTGCTGTATTACATTAAGG	
c-myc	Forward: GTCAAGAGGCGAACACACAAC	162
	Reverse: TTGGACGGACAGGATGTATGC	
TERT	Forward: AAATGCGGCCCCTGTTTCT	76
	Reverse: CAGTGCGTCTTGAGGAGCA	

Figures
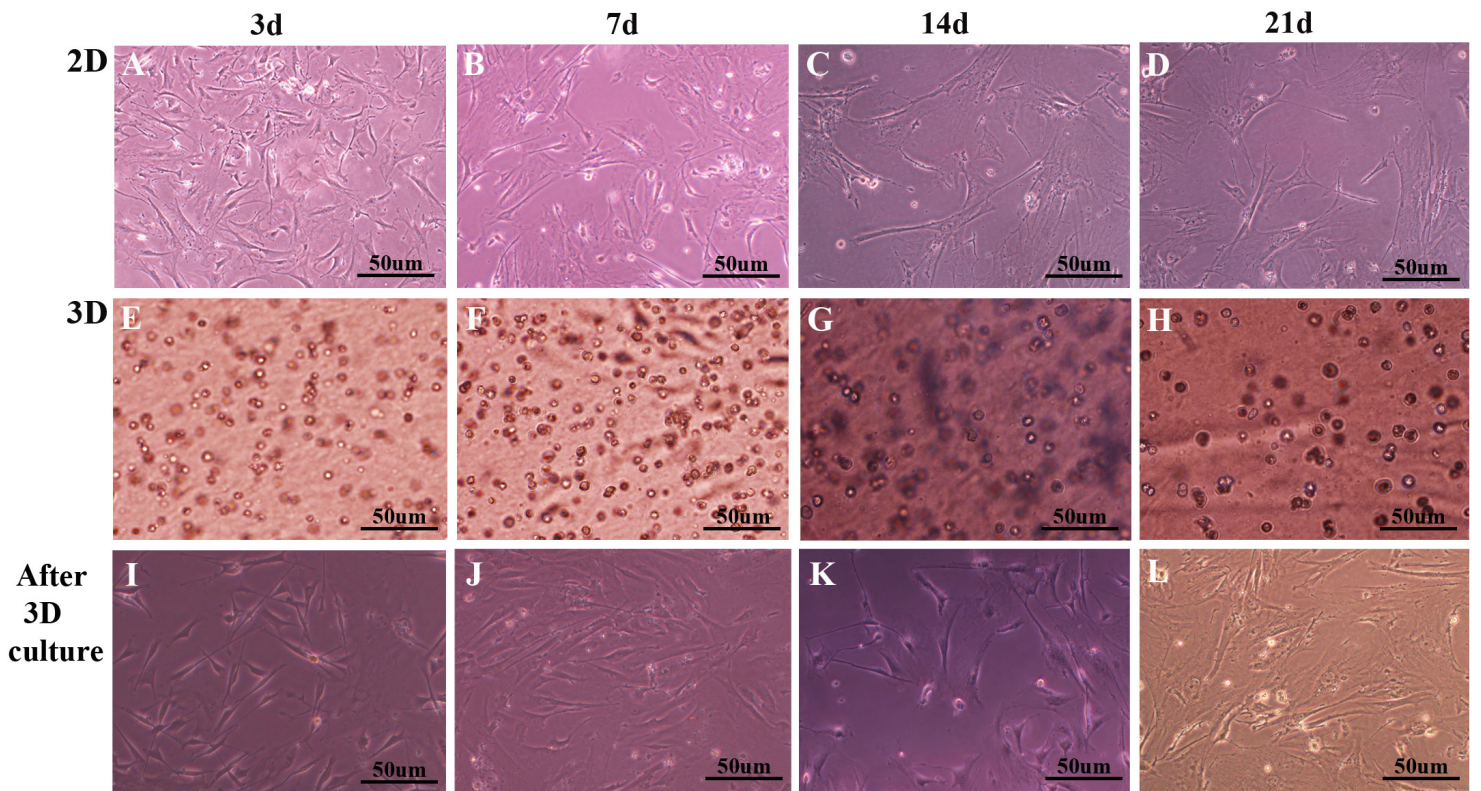
Figure 1

ADMSCs from the third passage were cultured in 2D and 3D cultures. a b At 3 d and 7 d, cells were relatively homogeneous, they had characteristic spindle-shapes and had smooth cell surfaces. c At 14 d, cells still maintained the characteristic MSCs shape, but some cells appeared to have pseudopod-like structures, and were longer and flatter. d At 21 d, cell shape was flat, and almost all ADMSCs lost their MSCs shape, cells were focal aggregation and exhibited a "fried egg" morphology. e f g h For 3D culture, most cells were round in shape and the cell density gradually increased. g h At 14 d and 21 d, some cells appeared to adhere to the vessel wall. i j k l Cells re-adhered to the vessel wall after 3D culture for 3 d, 7 d, 14 d and 21 d, respectively. The cell shape gradually became longer and flatter, but most cells maintained elongated spindle-shapes and had smooth cell surfaces. Cells never lost their characteristic MSCs shape. The experiment was repeated three times.
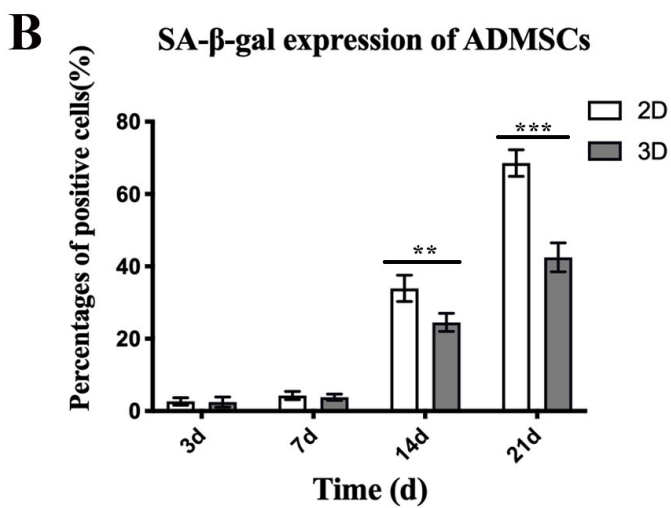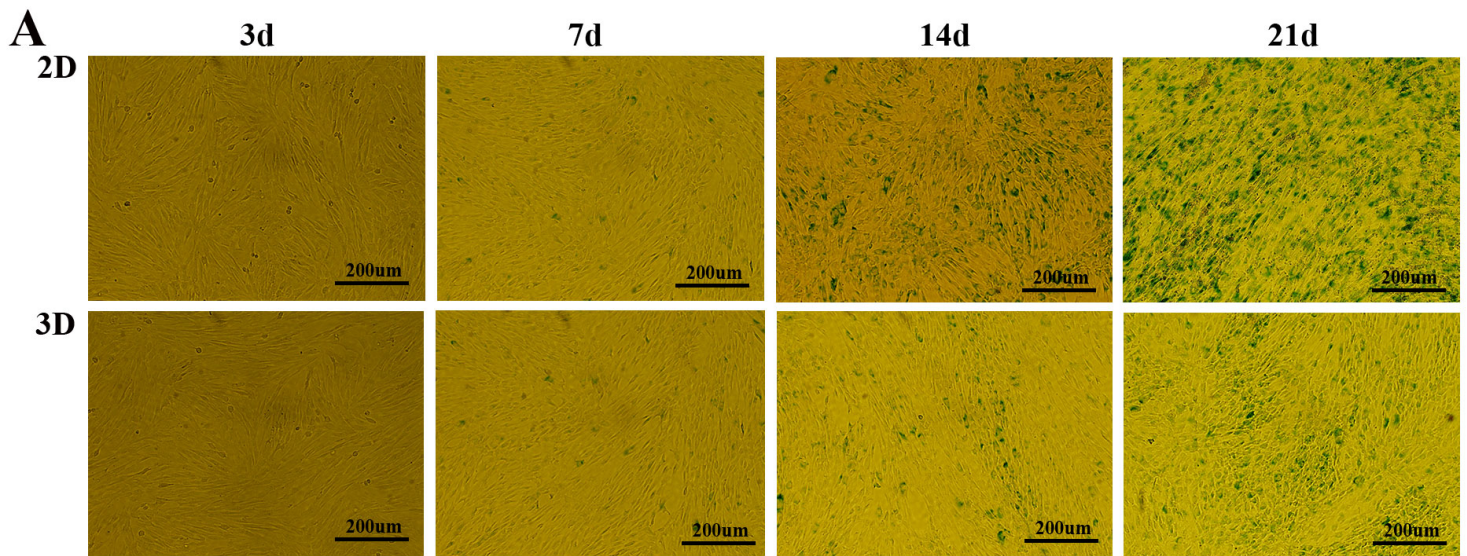
Figure 2

The expression of senescence-associated β-galactosidase in 2D and 3D ADMSCs culture. a b Little or no SA-β-gal expression was detected at 3 d and 7 d in either cultures, but increased expression was observed during progressive cultivation with time. Blue ADMSCs in 2D culture were statistically higher than 3D cultures at14 d. At 21 d, most ADMSCs were stained blue in 2D culture, but limited cells were stained blue in 3D culture at the same time period. Data represented as average ± SD from n = 3 experiments, **p◻0.01, ***p◻0.001.
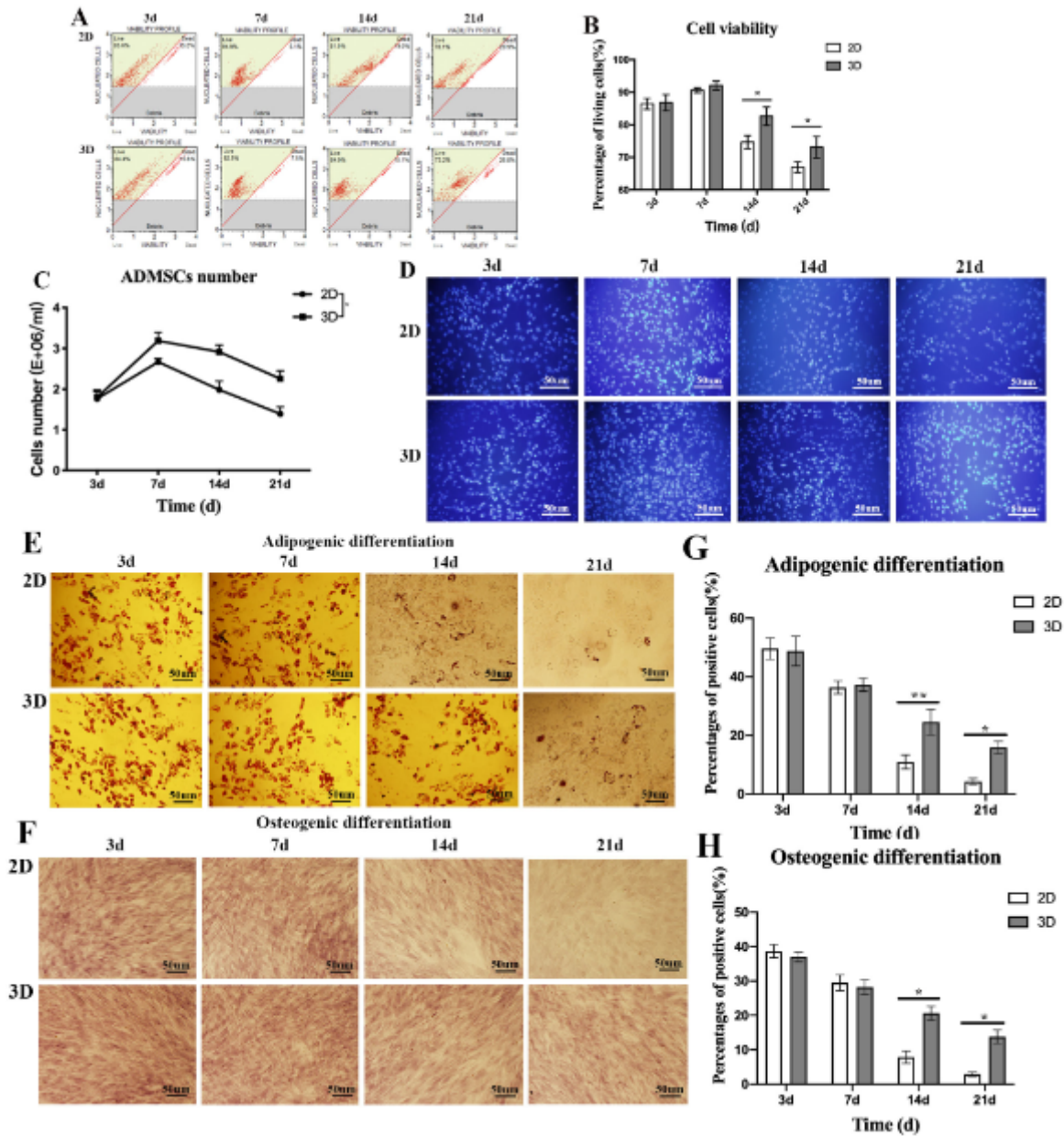
Figure 3

Cell viability of ADMSCs in 2D and 3D cultures at different time points. a ADMSCs viability was comparable for both culture conditions up to 7 d. After this period, viability gradually decreased with time, and was significantly decreased in 2D cultures when compared to 3D. b Cell viability in 3D cultures was significantly higher than 2D cultures at 14 d and 21 d. c The cells number in 2D and 3D cultures at every measured time point was counted. The cells number was significantly increased within 7 d in 2D and 3D cultures, and the population doubling time was 6 d and 4 d respectively, subsequently, the number of cells decreased rapidly, especially in 2D culture. Obviously, the cells number in 3D cultures was significantly greater than that in 2D. d Analysis of ADMSCs staining showed that the number of living cells was basically in accordance with the result of cell viability. e f g h Differences in adipo- and osteogenic capacity of ADMSCs in 2D and 3D cultures at 3 d, 7 d, 14 d and 21 d. Adipo- and osteogenic differentiation potential of ADMSCs were similar at 3 d and 7 d, for both culture conditions. A significant

age-related decline was observed in differentiation capacities at 14 d and 21 d in 2D cultures when compared with 3D. Cells practically lost all osteogenic differentiation in 2D cultures at 21 d. Data represented as average ± SD from n = 3 experiments, *p⬚0.05, **p⬚0.01.
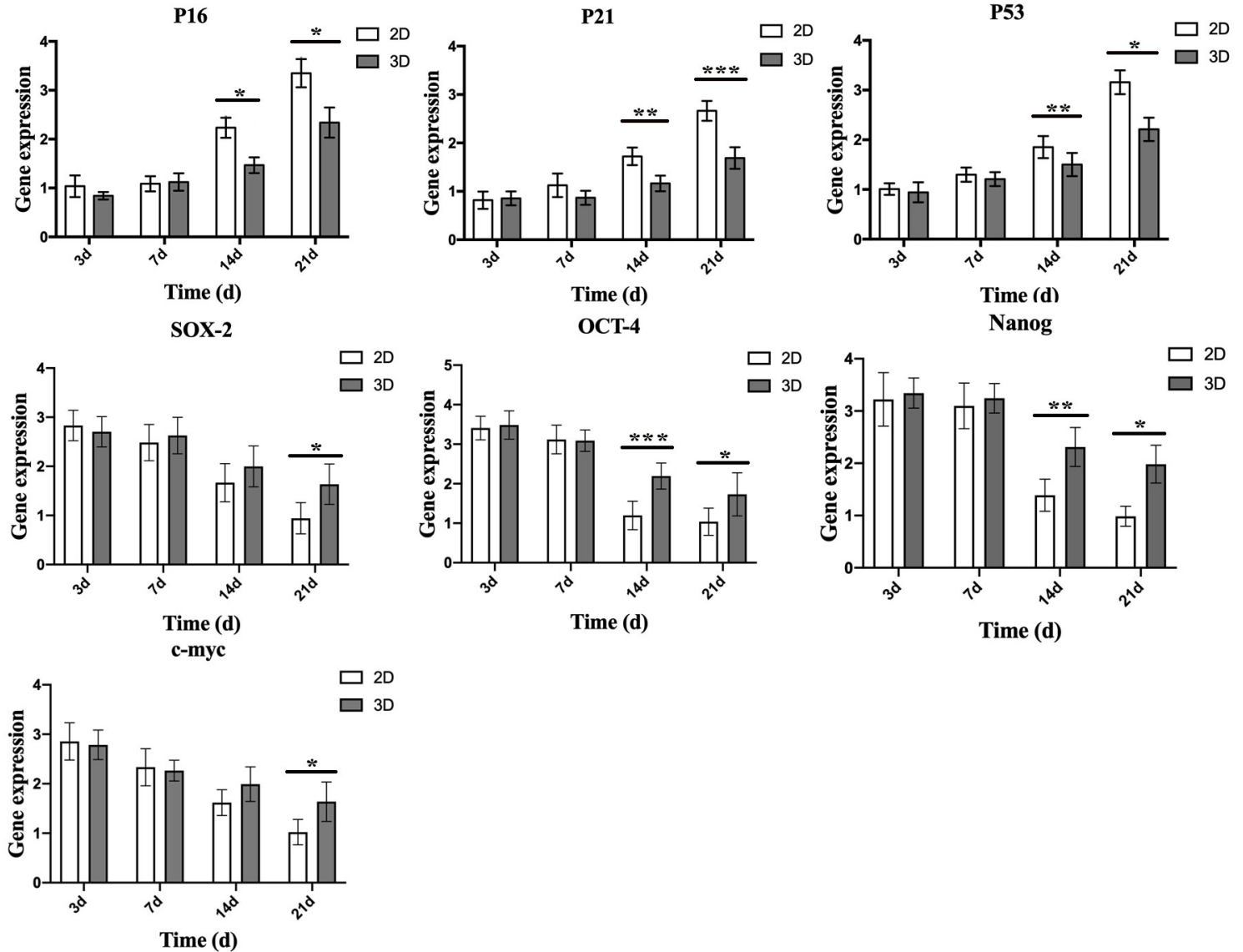
Figure 4

The expression of aging-related genes, p16, p21 and p53 gradually increased with culture time. The expression of all three genes in ADMSCs in 2D culture was significantly higher than 3D at 14 d and 21 d. In contrast, the expression levels of stemness-related genes, Sox2, Oct4, Nanog and c-myc exhibited a decreasing tendency. Moreover, Oct4 and Nanog expression exhibited a more significant reduction in 2D culture than 3D cultures at 14 d and 21 d, besides, Sox2 and c-myc expression were significantly decreased in 2D cultures at 21 d. Data represented as average ± SD from n = 3 experiments, *p⬚0.05, **p⬚0.01, ***p⬚0.001.
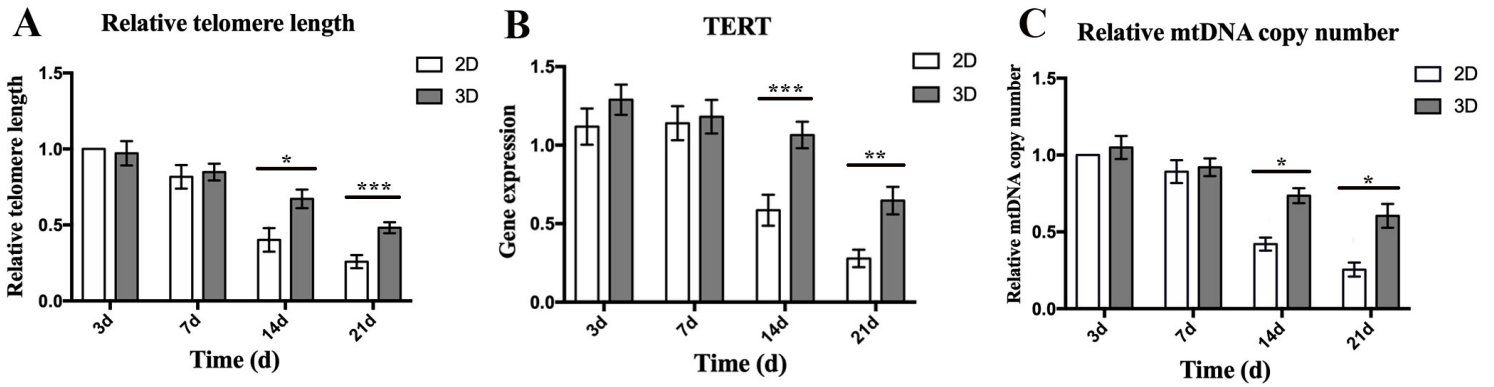
Figure 5

a Telomere length in ADMSCs gradually shortened during cell expansion in both 2D and 3D cultures. But telomere length shortened significantly in 2D cultures when compared to 3D, especially at 14 d and 21 d. Moreover, the shortening tendency in telomere length of ADMSCs in 3D cultures was steadier. b TERT expression revealed that changes in telomerase activity agreed with relative telomere length in ADMSCs for both cultures. c Relative mtDNA copy numbers in ADMSCs were gradually decreased, while mtDNA copy numbers in 3D cultures were significantly higher when compared with 2D cultures at 14 d and 21 d. Data represented as average ± SD from n = 3 experiments, *p≤0.05, **p≤0.01, ***p≤0.001.
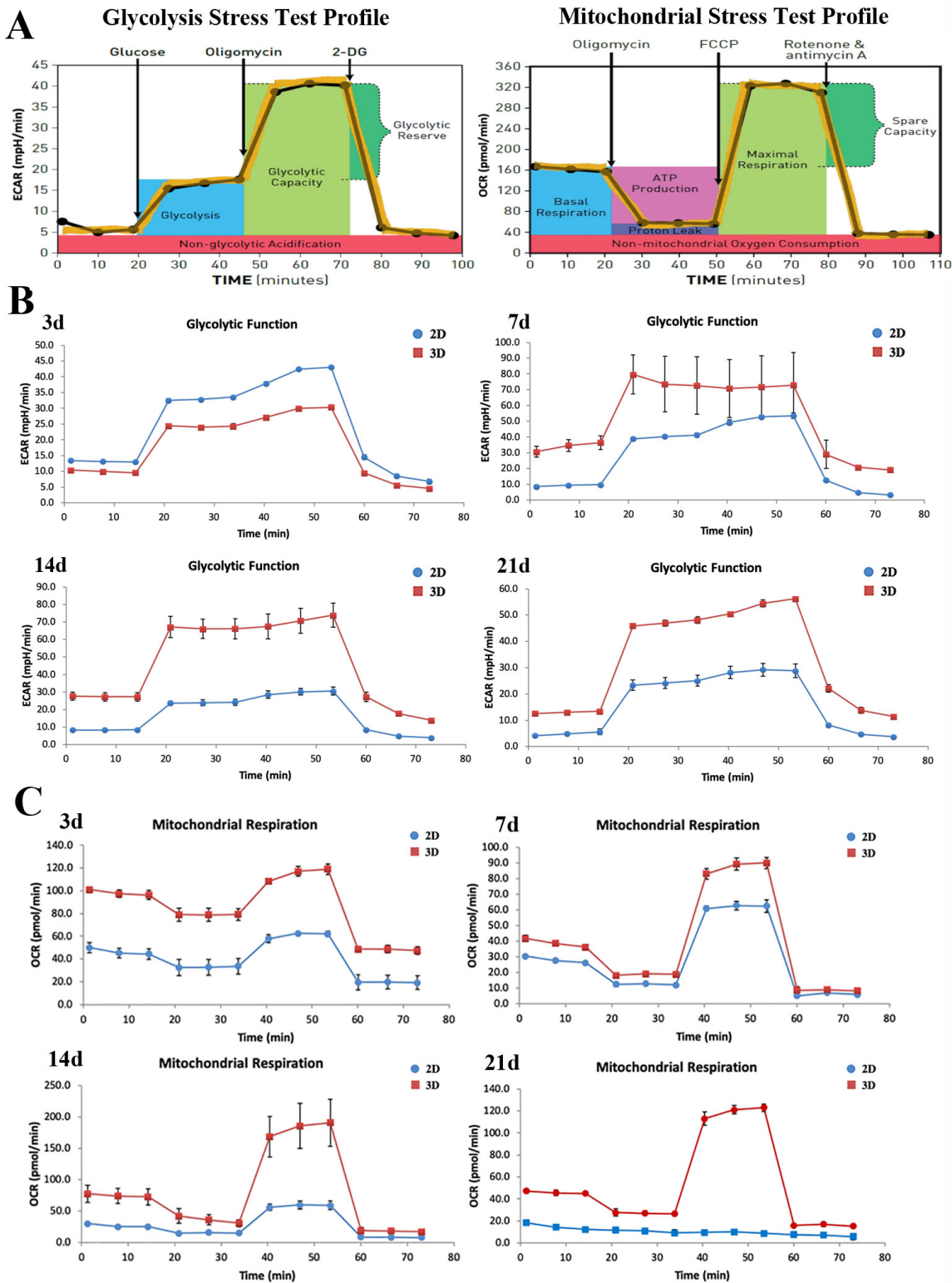
Figure 6

Change in glycolysis and mitochondrial respiration levels in ADMSCs. a Glycolysis and mitochondrial stress tests. b ECAR levels in ADMSCs in 3D cultures were higher than 2D cultures, at 7 d, 14 d and 21 d, but lower at 3 d. c OCR levels in ADMSCs in 3D cultures were higher when compared with 2D cultures at each time point. The experiment was repeated five times.